Journal of ELECTRONIC MATERIALS, Vol. 41, No. 7, 2012
DOI: 10.1007/s11664-012-1923-y

Shear Strength and Failure Modes of As-Bonded Gold and Copper Ball Bonds on Aluminum Metallization

C.D. BREACH[1,3] and T.K. LEE[2,4]

1.—ProMat Consultants, 160 Lentor Loop, #08-05 Tower 6, Singapore 789094, Singapore. 2.—ITE College Central, 20 Yishun Ave 9, Singapore 768892, Singapore. 3.—e-mail: cbreach@promat-consulting.com. 4.—e.mail: Lee_Teck_Kheng@ite.edu.sg

The shear test failure modes of "as-bonded" gold and copper ball bonds are fundamentally different. Soft gold balls are typically sheared by the tool, leaving a lower section of the ball bonded to the aluminum metallization. In contrast, copper balls do not undergo appreciable plastic deformation and are sheared completely away from the bond pad. Evidence is presented to show that the different failure modes of gold are copper are due to the relative strength of the balls. Copper balls are generally harder than gold balls, and the failure mode changes to the weakest interface, which is at the ball–aluminum bond pad. Gold ball bonds fail due to plastic deformation of the ball, while copper ball bonds fail by a process of plastic deformation in the aluminum bond pad.

Key words: Ball bond, intermetallic, gold wire, copper wire, fracture

INTRODUCTION

The high price of gold is causing the microelectronics industry to look for cheaper alternative materials for ball-bonded interconnects. A logical solution is replacement of gold with copper, because the electronics industry has extensive experience in use of larger-diameter copper wires (≥30 μm) in discrete and power devices. Copper wire has replaced gold in many low-pin-count packages for commercial applications[1,2] but has yet to be used in volume for fine- and ultrafine-pitch packages. Such packages typically use wire diameters in the range of 12 μm to 25 μm. The microelectronics industry is, however, looking into widespread adoption of copper wire, as highlighted by some recent studies.[3,4]

It seems inevitable that, as long as precious metals prices remain high, there will be increased focus on replacing gold and other noble metals with alternative materials, particularly for consumer electronics that do not require long operating life or high reliability. Reliability is, however, important for packages used in specific automotive, aerospace, military, and other reliability-sensitive applications. Introducing copper wire into such applications must be carefully planned, because it is more sensitive to moisture-induced failure than gold wire, as recent results have shown.[5–7] However, moisture-induced wire damage does not appear to be the cause of such poor reliability. Instead it seems to be caused by corrosion of intermetallics or the interfaces formed by intermetallics with the wire and the aluminum alloy bond pad.[8–10] In contrast, gold-aluminum intermetallics are relatively moisture resistant. An extensive experiential database of making gold perform well in fine-pitch, high-reliability applications is also a compelling reason why gold maintains a foothold in high-reliability electronics packaging.

Wire-bonded microelectronics packages are still evolving to ever finer pitches, and it is important to further explore and understand the reliability of gold and copper bonding wire in more detail than ever before so that designers and engineers can make informed decisions on when and how to use each material. The point of reference for characterizing the mechanical performance of these materials under various reliability test conditions is the performance of as-bonded balls. This brief article examines the shear failure modes of gold and

(Received October 8, 2011; accepted January 10, 2012; published online February 24, 2012)

copper ball bonds in the as-bonded condition, highlighting key differences between the two types of ball bond.

EXPERIMENTAL PROCEDURES

Ball bonds of nominal diameter 55 μm and height 13 μm were made with 2 N gold and 3 N copper wires on 1.2-μm-thick Al-0.5%Cu-1%Si bond pad metallization. Bonding was performed with an ASM Eagle 60AP wire bonder, and forming gas (95%N_2/5%H_2) was used with copper to prevent free air ball oxidation. Process optimization was performed using power (P), force (F), and time (t) as parameters, focusing on maximizing the shear strength. After optimum parameters were determined, a confirmation run was performed. A Dage 5000 series pull/shear tester was used for ball shear testing. Shear velocity was 300 μm/s, and shear height was 4 μm. Sample sizes of 20 balls were used for shear testing. Ball height and diameter are presented in Table I. Bonded balls were removed from bond pads by etching away the aluminum using a solution of KOH.[11] The topography of sheared bond pads of copper ball bonds was examined using a Digital Instruments Nanoscope IIIa scanning probe microscope operating in atomic force microscopy (AFM) mode.

RESULTS

Shear Tests and Fractography of As-Bonded Au and Cu Ball Bonds

Table II shows that the gold ball bonds had slightly larger shear strengths than the copper ball bonds. Optical images of typical failure modes of both types of ball bond are shown in Fig. 1 with schematics of the shear test. Figure 1a shows that the shear tool cuts through gold balls, shearing the upper section and leaving a lower portion of the ball attached to the bond pad. Figure 1b illustrates shearing of copper ball bonds away from the bond pad and failure at the ball–bond pad interface. Figure 2 shows a scanning electron microscopy (SEM) image of the surface of a typical aluminum bond pad after shear, which shows conic (parabolic) features, striations, and ligaments that are consistent with plastic deformation of aluminum. Examination of the underside of sheared balls in Fig. 3 shows that some aluminum remains on the ball, presumably adhered to intermetallics, while there are a few matt, relatively featureless regions that resemble brittle fracture surfaces.

Figure 4 shows SEM images of parabolic patterns on the underside of copper balls and the surface of the bond pad with illustrations of the shear test and the orientation of the conic features. The appearance

Table I. Dimensions of bonded gold and copper balls

Wire	Ball Height (μm)	Ball Diameter (μm)
Au	13.9 ± 0.3	54.8 ± 0.7
Cu	12.9 ± 0.27	56.8 ± 0.5

Table II. Shear strengths of bonded gold and copper balls

Measurement	Au	Cu
Mean	33.44	29.61
Median	33.41	29.64
Variance	2.40	1.03
Std. dev.	1.55	1.01

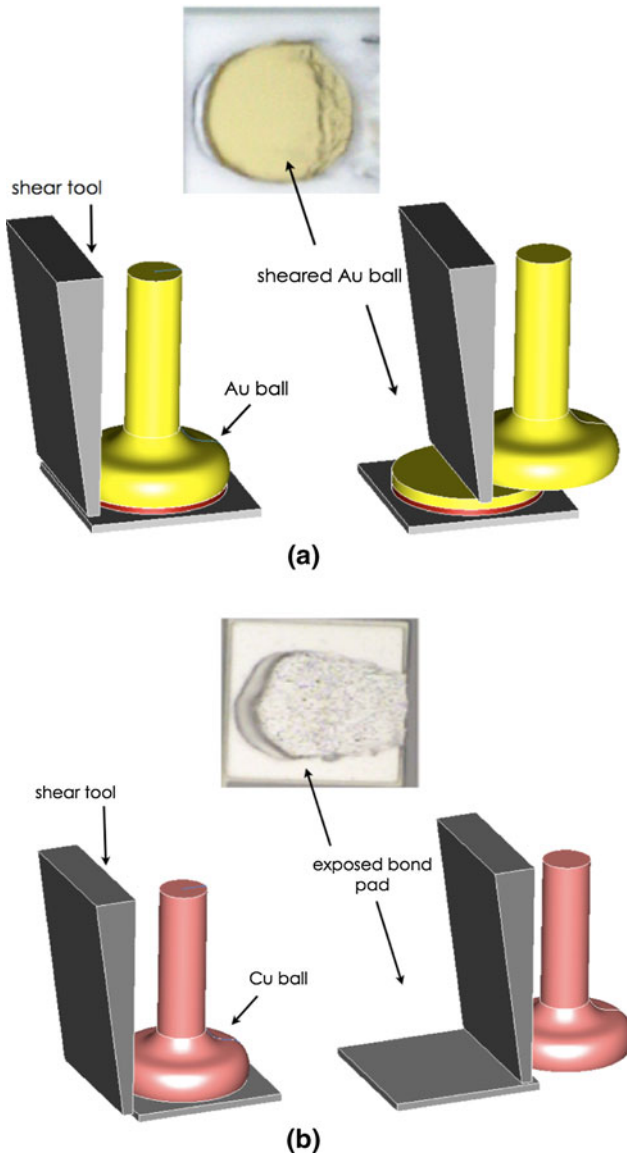

Fig. 1. Illustrations of shear test for as-bonded or aged balls: (a) plastic deformation and shearing of gold balls, (b) plastic deformation in aluminum and complete removal of copper balls from the bond pad; illustrations not to scale.

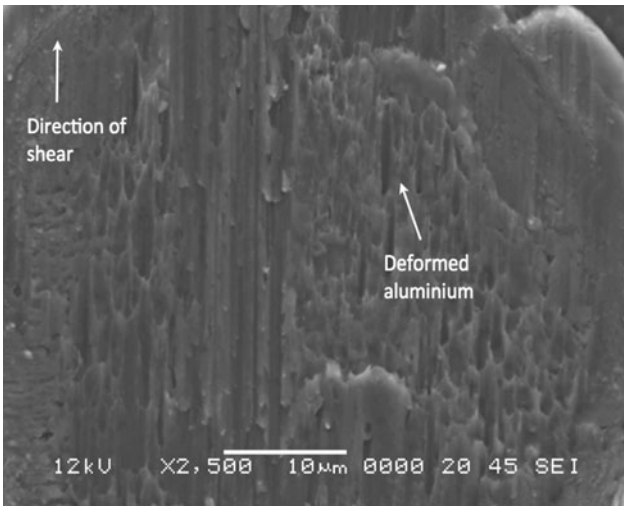

Fig. 2. SEM image of the chip side of a sheared as-bonded copper ball bond; note the striations in the aluminum due to plastic deformation.

Fig. 3. SEM image of the underside of a sheared as-bonded copper ball bond; note the striations in the aluminum due to deformation and regions that appear matt and featureless that are probably intermetallic or nonbonded regions of the ball.

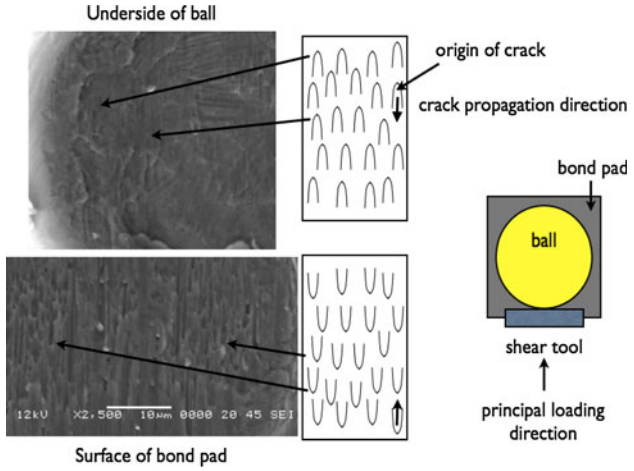

Fig. 4. SEM images of the underside of a copper ball bond and the surface of a bond pad after shear testing, highlighting the parabolic (conic) striations on the surfaces.

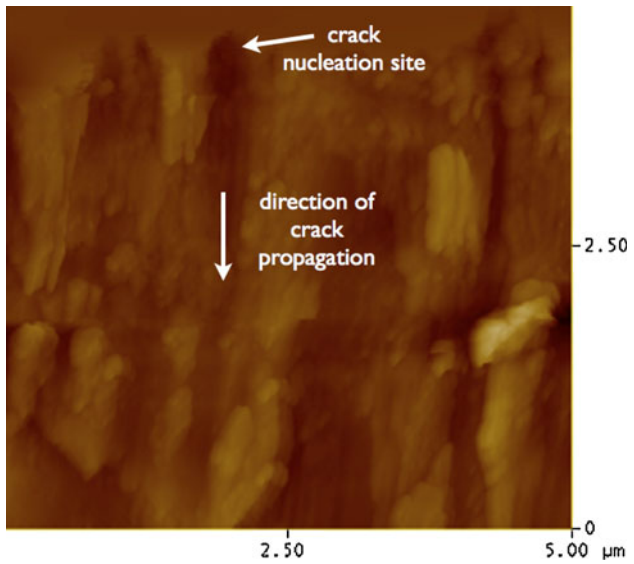

Fig. 5. AFM image of a typical region of the surface of a deformed aluminum bond pad after shear of copper ball.

of parabolic striations with opposite orientation is commonly observed on matching fracture surfaces of ductile metals that fail under mode II shear loading.[12,13] The areas around the vertex of each parabola are nucleation points of voids (cracks) that move towards the open end of the parabola, and each conic is a region where ductile crack movement was not uniform, with many cracks nucleated, arrested, and restarted during the shear test.[13] The parabolic features appear consistent with aluminum plastic deformation at the ball–bond pad interface, leading to the conclusion that copper ball bond strength is primarily due to plastic deformation of aluminum. A necessary condition to have strong copper ball bonds is therefore that the strength of bonding between the ball and aluminum and Cu-Al intermetallics is greater than the yield strength of the aluminum. Plastic deformation presumably takes place in a thin layer of aluminum at the intermetallic–bond pad interface. Figure 5 shows an AFM image of a small region of a typical deformed aluminum bond pad after shearing. The arrows indicate locations where ductile cracks are most likely initiated during shear testing. A three-dimensional AFM topographical image of the same region in Fig. 6 shows that the conic regions where cracks initiate and propagate are relatively shallow. Ductile crack propagation may start at nonbonded regions between the copper ball and aluminum bond pad (i.e., regions where there is not intermetallic coverage) that form cavities that can concentrate stress and initiate ductile cracks. Ductile cracks

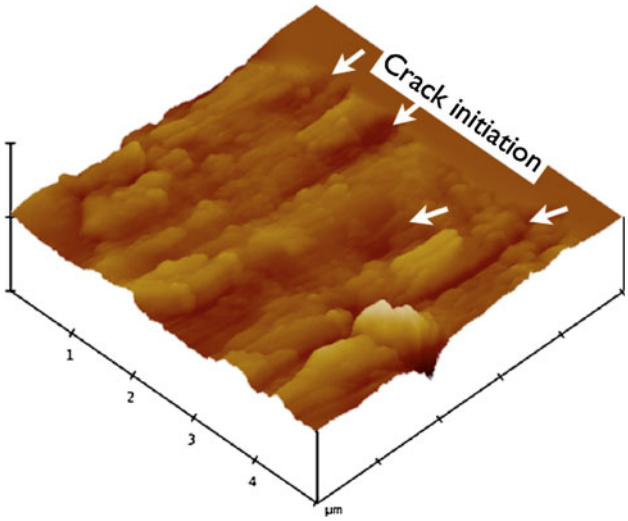

Fig. 6. AFM 3-D view of a typical region of the surface of a deformed aluminum bond pad after shear of copper ball.

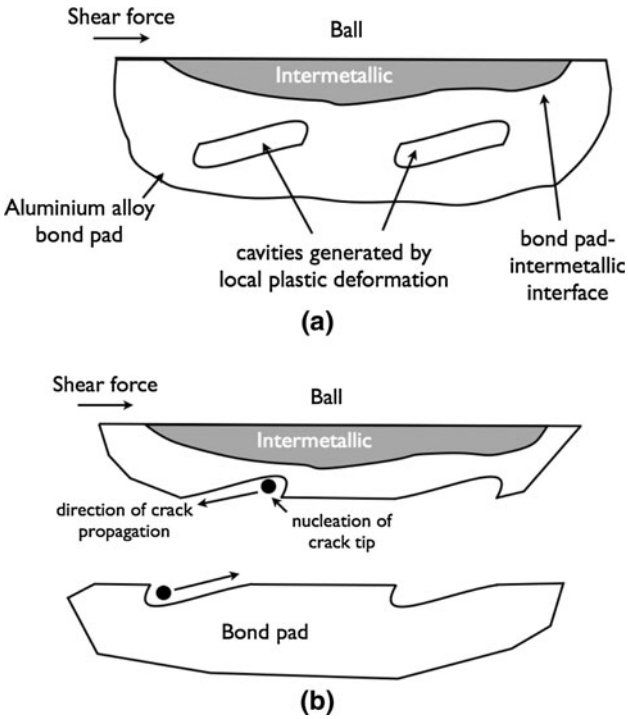

Fig. 7. Illustrations of (a) cavity formation during shear of copper ball on aluminum bond pad, (b) conic cavities developed during shear and after ball separates from the bond pad; adapted from Hull.[19]

may also nucleate within the bond pad at grain boundaries where inclusions, second-phase particles, and impurities may be present. Figure 7 shows a simple illustration showing that the conic shapes arise from elongation of cavities in the direction of the applied shear stress, which results in concentration of stress that reaches the yield stress of the aluminum, causing propagation of ductile cracks and orienting the cavities in opposite directions.

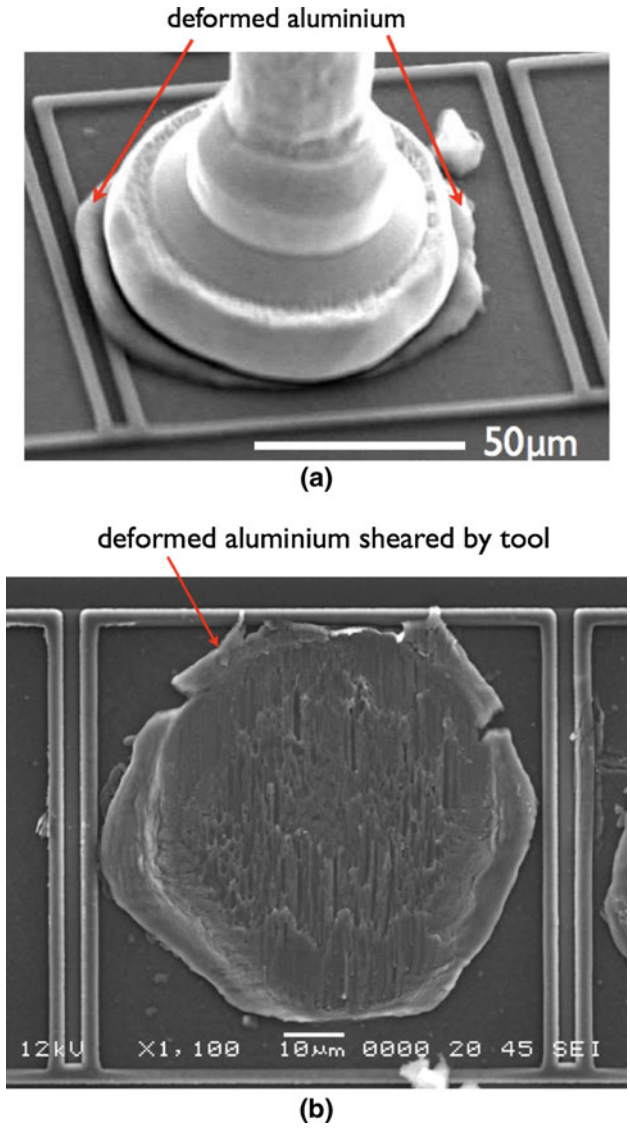

Fig. 8. (a) Typical example of an as-bonded copper ball bond showing plastically deformed aluminum at the ball periphery. (b) SEM image of the bond pad after shear testing, showing how the shear tool has cut through the deformed aluminum.

Copper ball bond strength can be affected by the presence of deformed aluminum around the ball periphery. Figure 8a shows an example of an as-bonded copper ball bond. The aluminum is deformed because harder copper wire requires higher-intensity ultrasound settings to deform the ball, which also are high enough to deform aluminum bond pads, resulting in the familiar aluminum "squeeze out" or "splash" as it is sometimes described. During shear testing the deformed aluminum may add additional resistance to shear and cause higher shear force readings, and Fig. 8b shows an example where the aluminum has been sheared either by the movement of the ball. The deformed aluminum layer is simply in mechanical contact with the ball periphery and is not bonded to the copper ball by

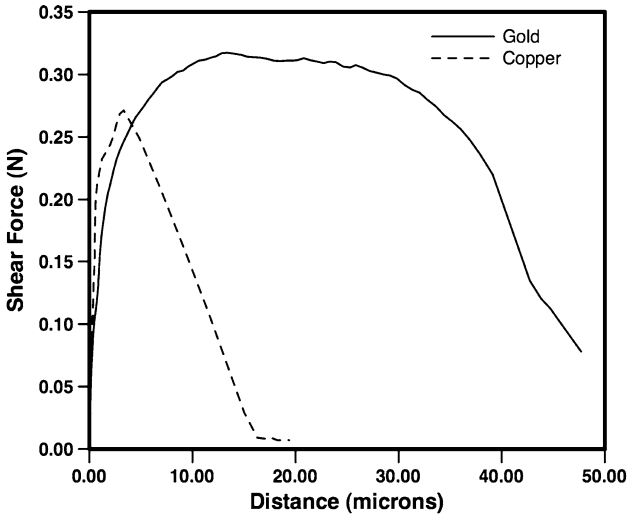

Fig. 9. Representative example force–displacement curves of gold and copper ball bonds.

intermetallic phases. This region of mechanical contact is curved and presumably is effectively a crevice or precrack where ductile cracks can also be initiated during shear testing.

Shear Force–Displacement Curves

Shear force–displacement data provide a useful tool that is sometimes used to characterize shear test consistency, being easily obtained because shear test equipment can be routinely set to record the data.[14] A representative example of a gold ball force–displacement curve in Fig. 9 shows that force was applied to the gold ball up to a distance of around 55 μm, almost the whole diameter of the ball. However, for copper wire, the force–displacement curve extends to approximately 20 μm, but the ball diameter was approximately 57 μm. Box plots of shear force in Fig. 10a show that the shear strength of gold balls was slightly higher than copper, the difference being on average around 2 g force. The work done during shear testing of ball bonds (denoted as the shear work) is shown in Fig. 10b; much more energy is expended in shearing gold balls compared with copper. Scatter plots of shear force versus shear work in Fig. 11 show that for gold there is an overall trend for higher shear force, accompanied by increased shear work. No such correlation appears to exist in the copper data. The results of linear regression analysis on these data are shown in Table III. The null hypothesis H_0 is that there is no correlation between shear work and shear force at significance level of $\alpha = 0.05$. The squared correlation coefficient R^2 for gold is 0.51, showing that there is significant correlation between shear work and shear force, which combined with the very low p value leads to the rejection of the null hypothesis and the conclusion that shear work and shear force are correlated for gold balls. With copper, however, R^2 is very low and the

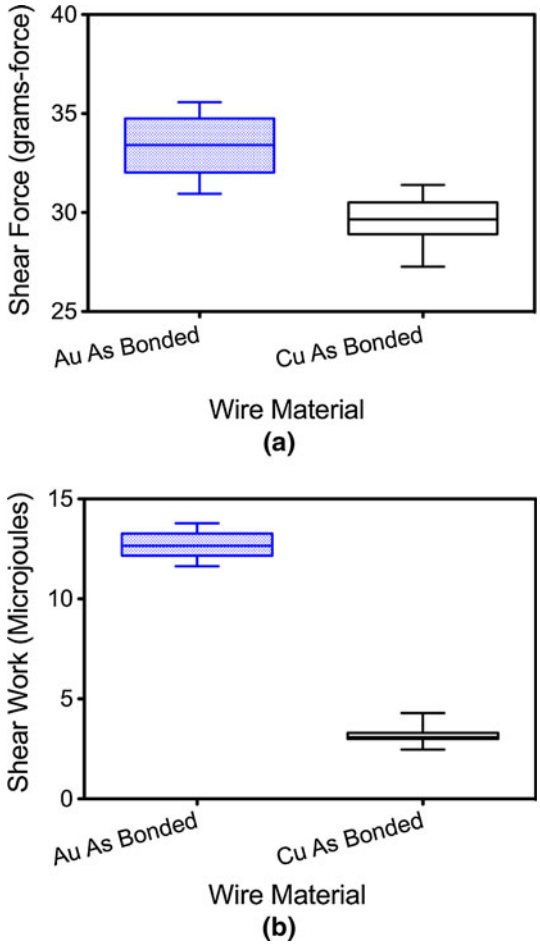

Fig. 10. Box plots of (a) shear force (sample size $n = 20$) and (b) shear work for gold and copper ball bonds.

p value is just slightly higher than the significance level, leading to the conclusion that there is no correlation.

The difference in the magnitude of the shear work for copper and gold is assumed to be related to the gold shear testing shearing through the ball, i.e., plastically deforming the gold ball, while shear testing of copper ball bonds involves plastic deformation of the thin layer of aluminum at the intermetallic–bond pad interface. The difference in energy presumably is due to the volume of plastic material being deformed, which in turn is a result of different deformation modes of gold and copper ball bonds. However, although the average shear force of gold balls is higher than copper, it should be possible to increase the shear force required to remove copper ball bonds from aluminum bond pads if a harder (stronger) bond pad is used.

Mechanical Analysis of Shear Test Data

Mechanical and finite-element analyses of ball shear testing are rare in wire bonding, with considerably more, but limited studies on solder ball shear tests.[15–17] An approach that can be applied to

ball bonds[15] considers the apparent fracture force (AFF) F_A, which is the peak force measured in the shear test from graphs such as those in Fig. 9, the force that plastically deforms the ball F_D, and the interfacial fracture force F_I. According to Bang et al.,

$$F_A(U_F) = F_D(U_F) + F_I, \quad (1)$$

where U_F is the distance at which the peak force F_A occurs in the shear force–distance curve. This equation is then rewritten[15] as

$$F_A(U_F) = \pi \sigma_Y D_B U_F + F_I, \quad (2)$$

where σ_Y is the tensile yield strength of the bump or ball material and D_B is the ball diameter. In solder balls, failure frequently tends to occur between intermetallics and the solder ball, which is similar to the failure mode also observed with copper ball bonds. Assuming yield strengths for each ball material based on literature data (or measurement if it can be performed), the ball diameter, and the distance at which the peak force occurs, it is possible to calculate the various forces. However, unless the distances over which the forces act are known, it is not possible to break the shear work into components, and therefore it is only possible to estimate the forces. The absence of coverage measurement is important here for copper because, while in solder joints it can be assumed that the whole contact area of the solder ball can be used (the balls are formed by melting on a pad of known diameter), with ball bonds the actual area is less than the contact area between the ball and the bond pad. Given that plastic deformation in aluminum only occurs where there is coverage, intermetallic coverage directly affects the fracture process in copper ball bonds, and greater coverage is expected to result in more plastic deformation and larger overall shear work. In gold ball bonds the interface is between two halves of the gold ball, a different situation than for copper ball bonds, and the interfacial force F_i appears to be a measure of the internal shear strength of the gold ball. Assuming yield strengths of 70 MPa for gold and 100 MPa for copper and using the ball diameters given in Table I, the forces can be estimated and are shown in Fig. 12. The results indicate that more force is used in plastically deforming the softer gold ball than the copper ball and that the interfacial force is larger in copper than in gold. Using

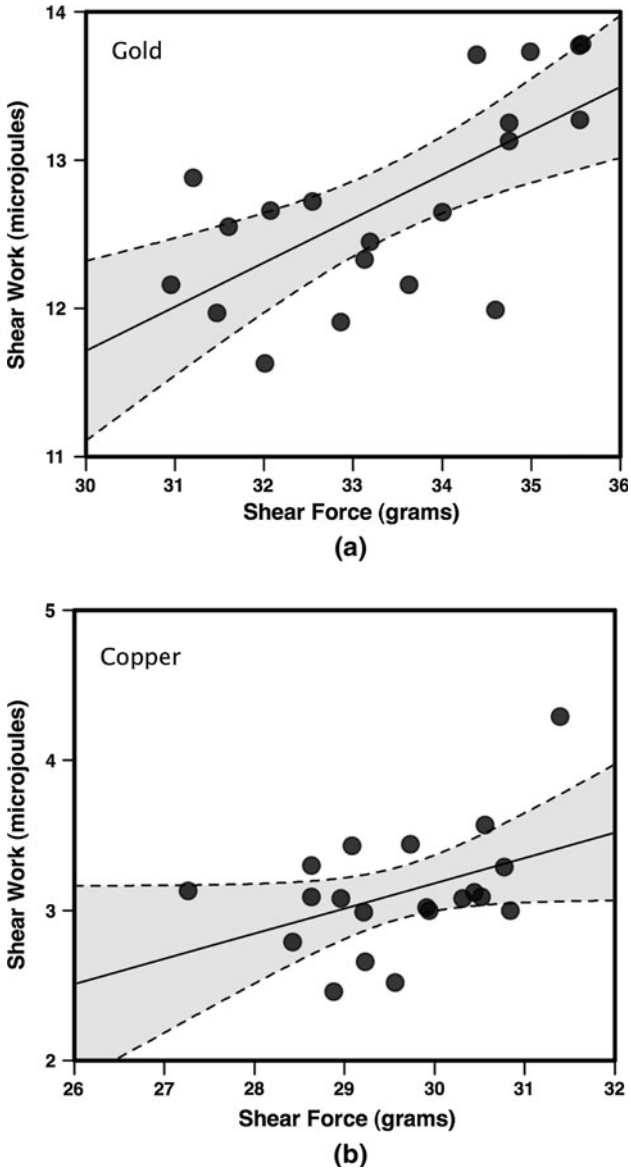

Fig. 11. Scatter plots of shear force and work for (a) gold ball bonds and (b) copper ball bonds.

Table 3. Regression analysis results of gold and copper ball bond data in Fig. 11

Source	Sum of Squares	Degrees of Freedom	Mean Square	*F*	*p*
Gold ball bonds: R^2 = 0.453					
Regression	3.998	1	3.999	14.899	0.01
Residual	4.823	18	0.268		
Total	8.830	19			
Copper ball bonds: R^2 = 0.185					
Regression	0.555	1	0.555	4.07	0.059
Residual	2.452	18	0.136		
Total	3.00	19			

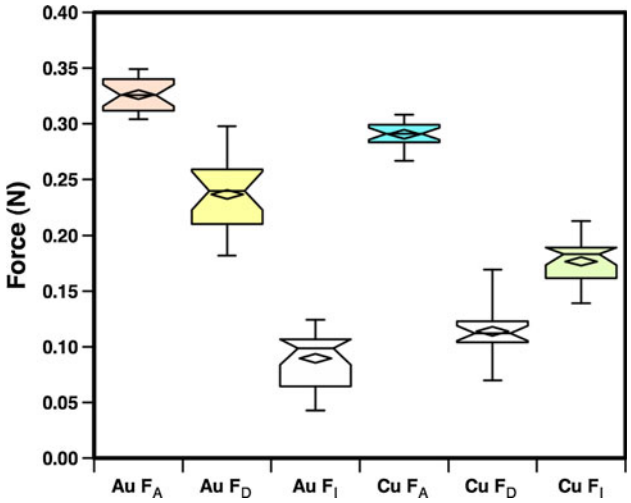

Fig. 12. Notched box plots of forces determined by assuming gold yield strength of 70 MPa and copper yield strength of 100 MPa with average ball diameter from Table I and U_F measured from the force–displacement graphs of each ball bond.

different values of the yield strength can change the various forces, but this simply shifts the relative magnitude while still resulting in the same overall appearance of the graph in Fig. 12. The usefulness of this approach with copper appears limited because of the lack of information on coverage, but conversely, calculation of F_i may allow indirect estimation of the amount of coverage at the interface. The larger the coverage, the greater the amount of plastic deformation between the intermetallic and the bond pad, and therefore F_i might be expected to be higher, although this is speculative at present.

DISCUSSION

The failure modes of ball bonds are determined by the relative strengths of the ball, the ball–intermetallic and intermetallic–bond pad interfaces, the intermetallics, and the aluminum alloy bond pad. The strongest materials in gold and copper ball bonds are the intermetallics, and the source of strength, as in many intermetallics, is the highly ordered crystallographic structures of these materials characterized by chemical bonding that may be a mixture of covalent, ionic, and metallic bonding.[18,19] From a simplistic viewpoint, mixed bonding occurs via charge transfer between the elements within the intermetallic, often involving *d* charge transfer from the noble element to aluminum and s charge transfer from aluminum to the noble element, with some internal shuffling of electrons among energy levels within each element. This has been the conclusion from studies on bulk and thin-film compounds.[20–26] The net result of the electronic interactions between the various elements would normally be seen in the strength of these materials, but the only strength data that appear to be available on intermetallics are for the high-temperature plastic strength of $CuAl_2$, which reaches levels of around 300 MPa at 375°C and increases at lower temperatures.[27] However, the hardness of Au-Al and Cu-Al compounds is a relative measurement of strength, and data in Tables IV and V for Au-Al and Cu-Al compounds,[28] respectively, clearly show that the intermetallics are much harder than wires and aluminum. A consequence of mixed bonding, especially from the covalent character, is that intermetallics are often very brittle, but in as-bonded gold and copper ball bonds, this is of no consequence because the intermetallics are normally void free.

Given the high strength of intermetallics in as-bonded ball bonds, it is the ball–intermetallic and intermetallic–bond pad interfaces that determine the mechanical strength. Chemical bonding between the ball metal, bond pad metal, and intermetallics is probably similar to the bonding within the elements of the intermetallic but is not generally understood. The dominant intermetallic in as-bonded gold ball bonds is typically a rather thick layer of Au_8Al_3. In gold ball bonds the strength of the chemical bonding at the intermetallic–metal interfaces and the intrinsic strength of the aluminum alloy bond pad are clearly higher than the strength of the gold ball, such that the tool simply shears through the gold ball. However the situation with copper ball bonds is more complex. As-bonded copper ball bonds may contain three main intermetallic compounds: $CuAl_2$ adjacent to the bond pad, and Cu_9Al_4 and possibly CuAl near the copper ball.[29,30] Figure 13 illustrates some possible interfaces that may occur in copper ball bonds with $CuAl_2$ and Cu_9Al_4 (CuAl is not included for brevity). As Fig. 13 illustrates, there are several interfaces in copper ball bonds. The aluminum bond pad is weaker than the intermetallic phases and the copper ball, and with strong bonding between aluminum and intermetallics, the main failure mode is ductile failure in aluminum, as seen in the AFM images of Figs. 5 and 6 as shallow conic features. Figure 14 illustrates with crystallographic representations how aluminum must remain well adhered to the intermetallic if plastic deformation is to occur within the aluminum bond pad. However, the presence of multiple intermetallics introduces the possibility of intermetallic–intermetallic interfaces, which must also be strongly bonded if ball bonds are to be mechanically robust. The cause of the matt regions seen in Fig. 4 is probably a result of brittle fracture between intermetallics as illustrated in Fig. 15, and presumably at these particular points, intermetallic–intermetallic interfacial strength is weak. A possible cause of weakness is the development of stresses between intermetallics during bonding due to molar volume differences between compounds. Tables IV and V present estimates of the molar volumes of Au-Al and Cu-Al compounds. Differences between the molar volumes of intermetallics can be quite large in both systems, but in as-bonded

Table 4. Composition ranges and hardness of Au-Al intermetallic compounds measured at ambient temperature

Phase	Composition (at.% Au)	Hardness HV5	Molar Mass (g)	Density (g/cm^3)	Molar Volume (cm^3)
Al	0–0.06	20–50	26.98	2.69	10.03
$AuAl_2$	32.92–33.92	263	250.92	7.5	33.46
AuAl	50	249	223.94	10.7	20.92
Au_2Al	66.3–66.7	130	420.90	13.7	30.72
Au_8Al_3	72.73	271	1656.62	14.9	111.18
Au_4Al	80	334	814.82	16.2	50.29
Au	84–100	60–90	196.96	19.3	10.19

Table 5. Composition ranges and hardness of Cu-Al intermetallic compounds measured at ambient temperature

Phase	Composition (at.% Cu)	Hardness HV5	Molar Mass (g)	Density (g/cm^3)	Molar Volume (cm^3)
Al (β)	0.0–2.84	20– 50	26.98	2.69	10.03
$CuAl_2$ (θ)	31.9–33.0	324	117.51	4.36	26.95
CuAl (η_2)	49.8–52.3	628	90.53	2.7	33.53
Cu_4Al_3 (ε_2)	55.2–56.3	616	335.13	NA	NA
Cu_3Al_2 (δ)	59.3–61.9	558	244.60	NA	NA
Cu_9Al_4 (Υ_2)	62.5–69	549	679.84	6.85	99.25
Cu (α)	80.3–100	60–100	63.55	8.93	7.12

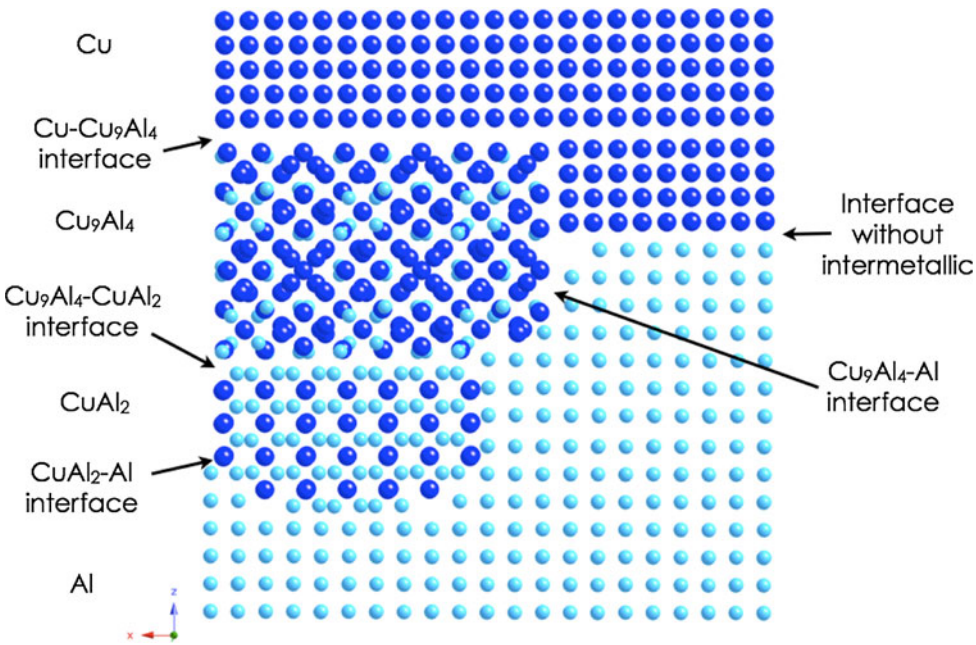

Fig. 13. Illustrations of some of the interfaces that may exist in copper ball bonds. Large spheres are copper; small spheres are aluminum. Note that the intermetallics in the illustrations have been drawn with a certain orientation only for the purposes of illustration; actual orientation may be different.

gold ball bonds the dominant phase is often Au_8Al_3, and when a single intermetallic is dominant, there is not an issue with differences between molar volumes. However, if intermetallics are in contact as in copper ball bonds, large differences in molar volumes may create stresses that weaken the interfaces, and Table V shows that the molar volume difference between Cu_9Al_4 and $CuAl_2$, two of the more commonly reported compounds in copper ball bonds, is rather large.

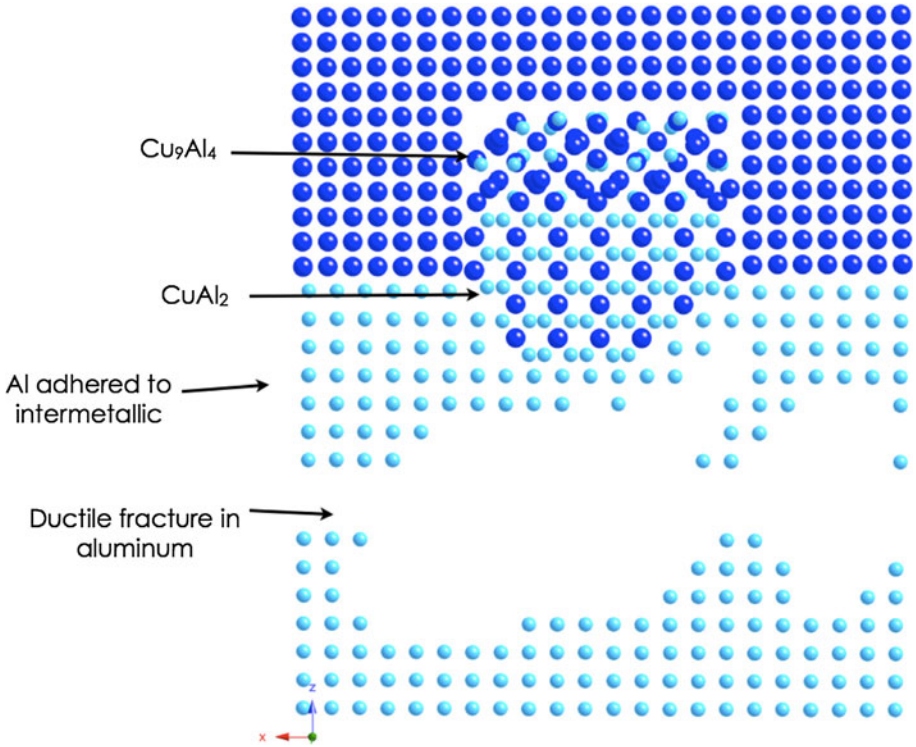

Fig. 14. Illustration of ductile fracture (tearing) of aluminum strongly bonded to intermetallics.

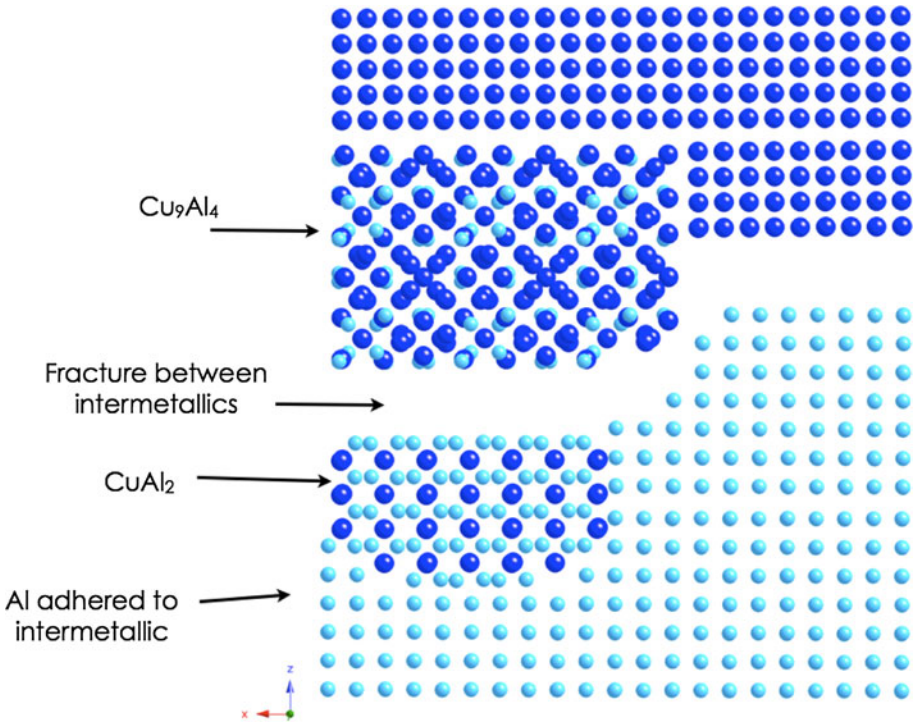

Fig. 15. Illustration of brittle fracture between intermetallics in a copper ball bond.

Although the difference in shear strength of gold and copper ball bonds is only a couple of grams-force, the difference in the amount of energy required to remove ball bonds is significant. The much smaller average shear work of copper ball bonds may be related to the amount of coverage, if it

is assumed that shear work is due only to plastic deformation of aluminum that is well bonded to intermetallics. Presumably, higher coverage would result in more deforming regions of aluminum and an increase in the shear work, but this was not confirmed in this study because it was not possible to estimate intermetallic coverage. There is, however, a complicating factor that may cause the apparent shear force and the shear work to be overestimated, namely the presence of squeezed-out aluminum at the ball periphery that does not contribute to the true interfacial bond strength. The plastic deformation of the deformed aluminum bond pad also requires additional work to be performed that is not related to the intermetallic coverage. Another result that may be affected by the deformed aluminum ring around copper ball bonds is the relationship between the shear force and shear work. In gold ball bonds there appears to be correlation between the shear work and shear force, but the lack of correlation between these measurements in copper ball bonds seems counterintuitive and may be due to the plastic deformation of the aluminum ring obscuring the true relationship between the shear work and shear force.

The mechanical analysis, though crude because of the assumed material properties, does seem to confirm what is seen in the shear test, i.e., that copper has much smaller deformation force due to the higher stiffness of copper balls relative to gold and a larger interfacial force component that may represent the scale of plastic deformation at the interface between the ball and aluminum bond pad. The analysis is too simplistic to assign great significance to the various force components, but the results may be interpreted such that, in copper ball bonds, larger interfacial force F_I may be equated to higher coverage, although clearly it is desirable to eliminate the effect of the squeezed-out aluminum to establish whether such a relationship is true.

CONCLUSIONS

Copper and gold ball bonds on aluminum metallization, bonded under optimum conditions that maximize intermetallic coverage, normally show fundamentally different failure modes during shear testing. Gold ball bonds are relatively soft compared with the bond pad, and the shear tool removes the upper part of the ball, leaving the lower part of the ball adhered to the bond pad. Copper balls are generally harder than gold and are sheared off the soft aluminum metallization with failure occurring by plastic deformation in the soft bond pad. The work done in shearing gold balls in this study was slightly larger than for copper balls of the same diameter under the same test conditions, which is probably due to a combination of deformation of the soft ball on contact with the tool and plastic shearing through the ball. In copper balls in this study the volume of aluminum undergoing deformation is assumed slightly smaller and therefore requires less energy to yield. In copper ball bonds, shear strength and work will depend on the degree of intermetallic coverage because plastic deformation of aluminum can only occur where intermetallics are bonded to the aluminum. At constant intermetallic coverage, it is possible that stronger aluminum bond pads may increase the shear strength of copper ball bonds.

ACKNOWLEDGEMENTS

The authors thank Dr. Richard Holliday of the World Gold Council for funding this research program exploring the characteristics and limits of gold and copper ball bonding.

REFERENCES

1. F.W. Wulff, C.D. Breach, D. Stephan, K. Dittmer, and M. Garnier. *Proceedings of the SEMI Technology Symposium (STS)*, vol. 1 (2004), p. 35.
2. F.W. Wulff, C.D. Breach, D. Stephan, and K.J. Dittmer, *Electronics Packaging Technology Conference*, *2004. EPTC 2004. Proceedings of 6th* (2004), p. 348.
3. B.K. Appelt, L. Huang, Y.S. Lai, and S. Chen. *Electronic Packaging Technology and High Density Packaging (ICEPT-HDP). 2011 12th International Conference on* 1–3 (2011).
4. B.K. Appelt, A. Tseng, Y.-S. Lai, and C.-H. Chen, *China Semiconductor Technology International Conference 2011* (2011).
5. S. Kaimori, T. Nonaka, and A. Mizoguchi, *Adv. Packag. IEEE Trans.* 29, 227 (2006).
6. T. Uno, S. Terashima, and T. Yamada. *Electronic Components and Technology Conference, 2009. ECTC 2009. 59th* (2009), p. 1486.
7. T. Uno, *Microelectron. Reliab.* 51, 148 (2011).
8. C.D. Breach and R. Holliday. *Proceedings of 11th International Conference on Electronic Packaging Technology and High Density Packaging (ICEPT)* (2009).
9. C.D. Breach, H. Shen, T.W. Mun, T.K. Lee, and R. Holliday, *12th Electronics Packaging Technology Conference (EPTC)* (2010), p. 44.
10. C.D. Breach, H.S. Ng, and T.K. Lee, *China Semiconductor Technology International Conference 2011 (CSTIC)*, vol. 34(1) (2011), p. 831.
11. F. Wulff and C.D. Breach, *Gold Bull.* 39, 175 (2006).
12. Modes of Fracture (Chapter 2), *ASM Handbook*: *Fractography*, vol. 12 (USA, American Society for Materials, 1987).
13. D. Hull, *Fractography: Observing, Measuring, and Interpreting Fracture Surface Topography* (Cambridge: Cambridge University Press, 1999).
14. S. Murali, N. Srikanth, and C.J. Vath III, *J. Electron. Packag.* 128, 192 (2006).
15. W.H. Bang, C.U. Kim, S.H. Kang, and K.H. Oh, *J. Electron. Mater.* 38, 1896 (2009).
16. J.Y.H. Chia, B. Cotterell, and T.C. Chai, *Mater. Sci. Eng. A* 417, 259 (2006).
17. J.Y.H. Chia, B. Cotterell, and A.Y.H. Cheong, *Mater. Sci. Eng. A* 428, 67 (2006).
18. G.A. Botton and C.J. Humphreys, *Micron* 28, 313 (1997).
19. G.A. Botton and C.J. Humphreys, *Intermetallics* 7, 829 (1999).
20. S.R. Cain and C.G. Woychik, *J. Phys. Chem. Solids* 53, 253 (1992).
21. M.H. Frommer, *Surf. Sci.* 64, 251 (1977).
22. Y. Grin, F.R. Wagner, M. Armbruster, M. Kohout, A. Leithe-Jasper, U. Schwarz, U. Wedig, and H. Georg von Schnering, *J. Solid State Chem.* 179, 1707 (2006).
23. P. Palade, F.E. Wagner, A.D. Jianu, and G. Filoti, *J. Alloys Compd.* 353, 23 (2003).
24. H. Piao and N.S. McIntyre, *J. Electron Spectros. Relat. Phenom.* 119, 29 (2001).

25. H. Piao, N.S. McIntyre, G. Beamson, M.L. Abel, and J.F. Watts, *J. Electron Spectros. Relat. Phenom.* 125, 35 (2002).
26. W. Zhou, L. Liu, B. Li, Q. Song, and P. Wu, *J. Electron. Mater.* 38, 356 (2009).
27. T. Chanda and G.S. Murty, *J. Mater. Sci.* 27, 5931 (1992).
28. E. Zschech, *Chapter 6 of Baugruppern Der Technolgie Elektronik* (Technik, 1997).
29. T. Boettcher, M. Rother, S. Liedtke, M. Ullrich, M. Bollmann, A. Pinkernelle, D. Gruber, H.J. Funke, M. Kaiser, K. Lee, M. Li, K. Leung, T. Li, M. L. Farrugia, O. O'Halloran, M. Petzold, B. Marz, and R. Klengel, *Proceedings of the 12th Electronics Packaging Technology Conference (EPTC)* (2010).
30. M. Drozdov, G. Gur, Z. Atzmon, and W.D. Kaplan, *J. Mater. Sci.* 43, 6029 (2008).